THE ASTROPHYSICAL JOURNAL SUPPLEMENT SERIES, 129:421–429, 2000 July


# MID-INFRARED INTERFEROMETRY ON SPECTRAL LINES. I. INSTRUMENTATION

J. D. MONNIER,[1] W. FITELSON, W. C. DANCHI,[2] AND C. H. TOWNES
Space Sciences Laboratory, University of California, Berkeley, Berkeley, CA 94720-7450
*Received 2000 January 10; accepted 2000 March 2*

## ABSTRACT

The Infrared Spatial Interferometer at University of California, Berkeley has been outfitted with a filter-bank system to allow interferometric observations of mid-infrared spectral lines with very high spectral resolution ($\lambda/\Delta\lambda \sim 10^5$). This paper describes the design, implementation, and performance of the matched 32 channel filter-bank modules, and new spectral-line observations of Mars and IRC +10216 are used to demonstrate their scientific capability. In addition, observing strategies are discussed for accurate calibration of fringe visibilities in spectral lines, despite strong atmospheric fluctuations encountered in the infrared.

*Subject headings:* instrumentation: interferometers — instrumentation: spectrographs — techniques: interferometric

## 1. INTRODUCTION

The Infrared Spatial Interferometer (ISI) consists of two 1.65 m telescopes employing heterodyne detection between 9 and 12 $\mu$m using $CO_2$ lasers as local oscillators (LOs) (Hale et al. 2000; Lipman 1998). Observations can be made at a large number of frequency bands in this spectral range by tuning to the various lasing transitions of different $CO_2$ isotopes. The ISI has measured the characteristics (sizes and optical depths) of dust shells around late-type stars (e.g., Danchi et al. 1994) and angular diameters of the nearest red supergiants (Bester et al. 1996). In these cases, sensitivity to continuum (dust or photospheric) emission using heterodyne detection is generally less than that theoretically possible using direct (photon-counting) detection techniques, partly because the maximum bandpass is limited by the temporal response of the IR detector, which is about 5 GHz with present detectors ($\lambda/\Delta\lambda \sim 5000$).

However, for narrow bandpasses, heterodyne receivers are more sensitive than direct detection schemes, which are not background limited for low flux levels (see more detailed discussion by Monnier 1999 and Hale et al. 2000). Furthermore, extremely high spectral resolution is attainable with heterodyne spectroscopy (e.g., Betz 1977) since the down-converted astronomical signal can be further filtered with conventional radio-frequency (RF) filters. Such high resolution is needed to resolve many molecular lines that form in cool winds around asymptotic giant branch (AGB) stars ($\Delta v \sim 1$ km s$^{-1}$) or in planetary atmospheres. Betz was able to observe transitions of $CO_2$ around Mars and Venus with spectral resolution of $\lambda/\Delta\lambda \sim 6 \times 10^6$ (Betz et al. 1976). Interferometry with this resolution can hence measure the location and distribution of molecules in particular excitation states.

Naturally, the high spectral resolution potential of a heterodyne system can only be realized by using a spectrometer in the RF signal chain following detection, a capability that was not part of the original ISI design. Although previous systems have been built for high-efficiency spectral-line work with wide RF bandwidths on single telescopes (e.g., Betz 1977; Goldhaber 1988; Isaak, Harris, & Zmuidzinas 1999; Holler 1999), no system existed that was suitable for interferometry on narrow bands because of the need to correlate signals from two separate telescopes.

This paper will describe the implementation of an inexpensive filter-bank system for spectral line observations using the ISI. After a description of the filter bank itself, its performance will be evaluated from laboratory measurements and test observations of astronomical objects. Fluctuations from the turbulent atmosphere and unexpected instrumental drifts required new observing strategies for accurate calibration of the fringe visibility on and off spectral lines. These techniques are described in detail, including fast bandpass switching for phase referencing and LO switching for robust correlator calibration. Last, the near-term scientific potential of combining high spectral and spatial resolution at these wavelengths is reviewed.

## 2. THE 32 CHANNEL FILTER BANK

### 2.1. *Introduction*

In principle, heterodyne spectroscopy with an RF filter bank is quite simple, even at 27 THz. A $CO_2$ laser in each ISI telescope acts as an LO, with a wavelength of $\sim$11 $\mu$m. Wave fronts from the laser are mixed with light from the sky, and the resulting "beat" pattern is detected by an HgCdTe photodiode with a large output bandwidth ($\pm\Delta v$). This process is called "heterodyne" detection and down-converts a $2\Delta v$ bandwidth centered around 27 THz (mid-infrared radiation) into microwave signals between DC and $\Delta v$. In a double-sideband (DSB) system such as the ISI, frequencies both above and below the LO frequency are converted into the same (microwave) frequency, thus overlapping each other. When observing a spectral line, this has the undesired effect of diluting the line (in one sideband) with uninteresting continuum radiation (from the other sideband) but can still be readily interpreted when multiple spectral features are not overlapping.

Once the signals have been down-converted to microwave (or RF) frequencies, they are amplified by cold field effect transistor (FET) amplifiers and transmitted through coaxial cables. Tunable RF filters with bandwidths of 60 MHz (and much narrower) have been available for quite some time and can be used to filter the astrophysical signals.

[1] Current Address: Smithsonian Astrophysical Observatory MS #42, 60 Garden Street, Cambridge, MA 02138.
[2] Current Address: NASA Goddard Space Flight Center, Infrared Astrophysics, Code 685, Greenbelt, MD 20771.

Since the original frequency of the radiation was $\sim 27$ THz, the use of filters with 60 MHz bandwidth corresponds to a spectral resolving power of $\lambda/\Delta\lambda = 27$ THz/60 MHz $= 4.5 \times 10^5$, fine enough to resolve spectral features arising from Doppler shifts as small as $\sim 0.7$ km s$^{-1}$.

### 2.2. *Design Considerations*

Being a first generation instrument, the ISI filter bank had modest design goals:

1. Spectral resolution must be sufficient to resolve narrow absorption lines around AGB stars (a few km s$^{-1}$).
2. Full bandpass must be broad enough to encompass both the relevant absorption line and significant bandwidth of the continuum ($\sim 2$ GHz).
3. Because of high demand for ISI continuum observations, the filter-bank system should minimally interfere with standard observing, i.e., it should not involve a radically different hardware configuration.
4. A fast bandpass-switching scheme to calibrate atmospheric fluctuations should be implemented.
5. Cost must be relatively low, i.e., no digital correlator.

Table 1 summarizes the technical features of the completed filter-bank system, satisfying all of the above design goals. The desire to minimally impact the current hardware design of the ISI imposed the most severe restrictions on the design. In order to maintain the current RF architecture behind the correlator and to avoid the development of an entirely new data acquisition system, spectroscopic capabilities were added to the ISI by inserting a filter-bank system before the correlator and total infrared power detection subsystems. Figure 1 shows a schematic of the major subsystems of the ISI, including the dual 32 channel filter bank. Detailed descriptions of the ISI itself can be found in the instrument paper by Hale et al. (2000) and in recent Ph.D. theses (Lipman 1998; Monnier 1999).

The interferometer must be able to measure not only the flux density of infrared radiation incident on both telescopes (i.e., the total IR power) but also the strength of the interference of signals from both telescopes (i.e., the fringe power). By filtering the RF signals from both telescopes with the two filter-bank modules before correlation, the infrared (IR) power and fringe signal could be measured in a manner identical to that used for the broadband (continuum) signal. When not performing spectroscopic observations, the filter bank can be switched out of the RF path through a bypass line inside each filter-bank module (see Fig. 2). This strategy has the distinct advantage of not impacting the existing hardware *at all* and also does not require any additional RF detection or data acquisition development. However, because the filter bank intercepts the RF signals before correlation, the two modules of the filter bank (one set of 32 filters for each telescope) must be phase matched. This imposed strict requirements on all of the RF components inside the filter bank and contributed significantly to construction complexity and component costs. The other important performance trade-off was that only one filter bandpass can be observed at a time, unlike typical spectrometers where detectors (e.g., RF diodes) are placed behind all filters and read out in parallel, allowing the entire spectral line to be measured at once. This limits the uses of the filter bank, for example, making it impractically slow to perform standard spectroscopic observations for a large number of lines.

TABLE 1

IMPORTANT SPECIFICATIONS OF ISI FILTER BANK

| Parameters | Specifications |
|---|---|
| Bandpass | 270–2190 MHz |
| Number of filters | 32 per telescope |
| Individual filter bandwidth (3 dB points) | 60 MHz |
| Spectral resolution at 11.15 $\mu$m | $\sim 0.7$ km s$^{-1}$ |
| Phase matching | $\pm 10°$ over 80% of band<br>$\pm 20°$ over entire band |
| Gain dynamic range | 15 dB |
| Bandpass switching rate | up to 500 Hz |

Figure 2 shows a detailed block diagram of one of the two filter-bank modules, with every major component in the RF chain. In order to filter the bandpass, the original RF signal from each telescope is split into 32 frequency bands via a four-way power splitter followed by four eight-way splitters. This decreases the signal power in each band by 15 dB, and amplification is applied before, during, and after this splitting to keep signal levels high enough that the additional amplifier noise from this part of the signal chain causes no significant decrease to the signal-to-noise ratio (S/N). In addition, custom frequency equalizers are used to maintain a reasonably flat frequency response throughout each module and within each submodule. After being split into 32 bands, the RF signals encounter the filters. Thirty-two switches are used to select the desired bandpass (any combination is allowed), after which the signals are recombined through a symmetric combination of four eight-way combiners and a single four-way combiner. Following recombination, the signal is amplified and any overall bandpass slope removed before finally being reinjected into the ISI system.

In order to make sure that the filter bank puts out as much RF power as it receives (net power gain of 0 dB) independent of the bandpass selected, a variable attenuator and amplifier are used in combination to provide up to 15 dB of relative amplification. This is done so that the laser shot noise always dominates the measurement noise and the final detection diodes are always used at similar power levels.

Onboard memory allows the storage of two separate bandpass selections, which can be switched back and forth rapidly either by a computer-controlled chop signal or by one from an external signal generator. This capability allows the measurement of both the narrow absorption line and the broad continuum on alternate chop cycles within an atmospheric coherence time, removing brightness fluctuations as a source of measurement uncertainty. Bandpass selection and gain/attenuator control can be accomplished via manual switching or through a computer interface. Presently, the filter-bank bandpass and gain selections are made using a C-language program running on a Sun workstation interfaced with the main ISI control computer.

### 2.3. *Performance*

Figure 3 shows the transmission of the two filter-bank modules of the completed filter bank. An ideal frequency response would be a flat transmission curve inside the allowed bandpass. However, a peak in the transmission occurs at overlapping band edges as a result of a design flaw in the individual filter bandpasses (see Monnier 1999 for

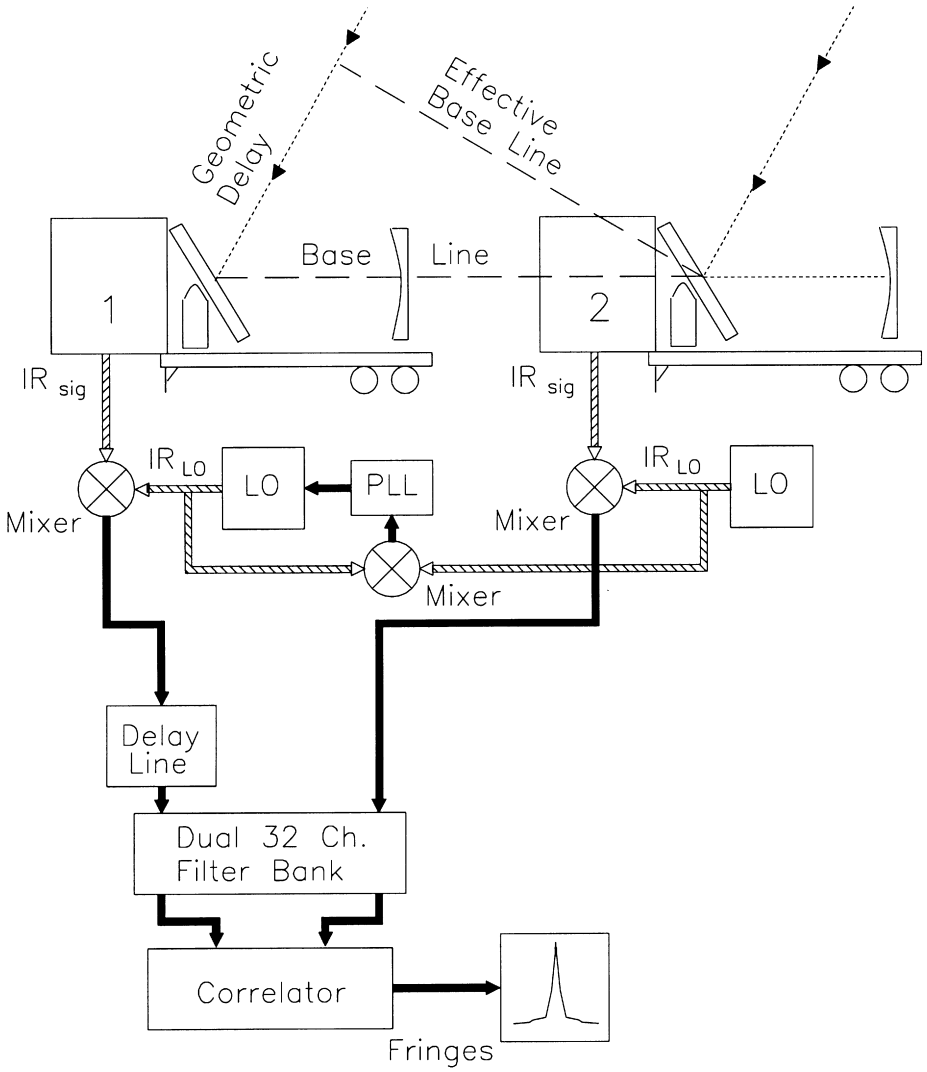


FIG. 1.—Block diagram of the ISI interferometer with the filter bank in the RF path. Two trailers, each containing a telescope, are indicated. IR signals are mixed with LO power from $CO_2$ lasers. After passing through a filter bank that determines the bandpass, the resulting RF signals from the two telescopes interfere in a correlator, producing interference fringes. The two LOs are kept in phase by a phase lock loop circuit. See Hale et al. (2000) for complete details.

further details). The net effect of this mismatch is a slight degradation of the S/N. This occurs because when the RF is finally detected in a diode, the signal adds up coherently as a function of frequency, while the noise adds up incoherently. In order to accurately estimate the effect on the S/N, the phase response of the system must also be characterized. A network analyzer has been used to measure the relative phase delay for RF signals propagating through the two modules of the filter bank. This "differential phase" response appears in Figure 4 and shows that the phase is matched to $\pm 10°$ over 80% of the bandpass and is always within 20°. Using this information, calculation (based on eq. [6.36] in Thompson, Moran, & Swenson 1986) shows that the filter-bank gain ripple only decreases the S/N by $\sim 10\%$ over most of the bandpass. Further discussion of the S/N degradation as a function of frequency can be found in Monnier (1999).

In order to confirm these calculations, S/N measurements were made at the telescope while observing a calibration hotbody source (373 K). The results can be found in Figure 5. The S/N was measured for a series of bandpass widths throughout the full frequency range. There are two major conclusions that can be drawn from these measurements. First, the S/N has the expected behavior as a function of bandwidth (S/N $\propto$ (bandwidth)$^{1/2}$). Secondly, the S/N of the filter bank, when extrapolated to the effective bandwidth of the normal ISI system ($\sim$2300 MHz), is $\sim 10\%$ low (expected S/N $\sim$ 500), confirming the theoretical expectation that the gain ripple causes only a modest loss in S/N.

## 3. OBSERVING METHODOLOGY

The filter-bank observing methodology described in this section allows a precise and accurate *relative* measurement of the infrared power in two bandpasses. The first, bandpass 0 (BP0), is usually only a few filters wide (to match the absorption-line width) while the second, bandpass 1 (BP1), is typically much larger (to make an accurate measurement of the continuum). The filter bank switches rapidly between these two bandpasses in order to calibrate signal fluctuations due to seeing and telescope guiding changes. This observing strategy makes the ratio of IR power in BP0 to BP1 insensitive to such sources of fluctuations.

Determining the final calibrated ratio of infrared power in BP0 compared to BP1 requires four nested levels of com-

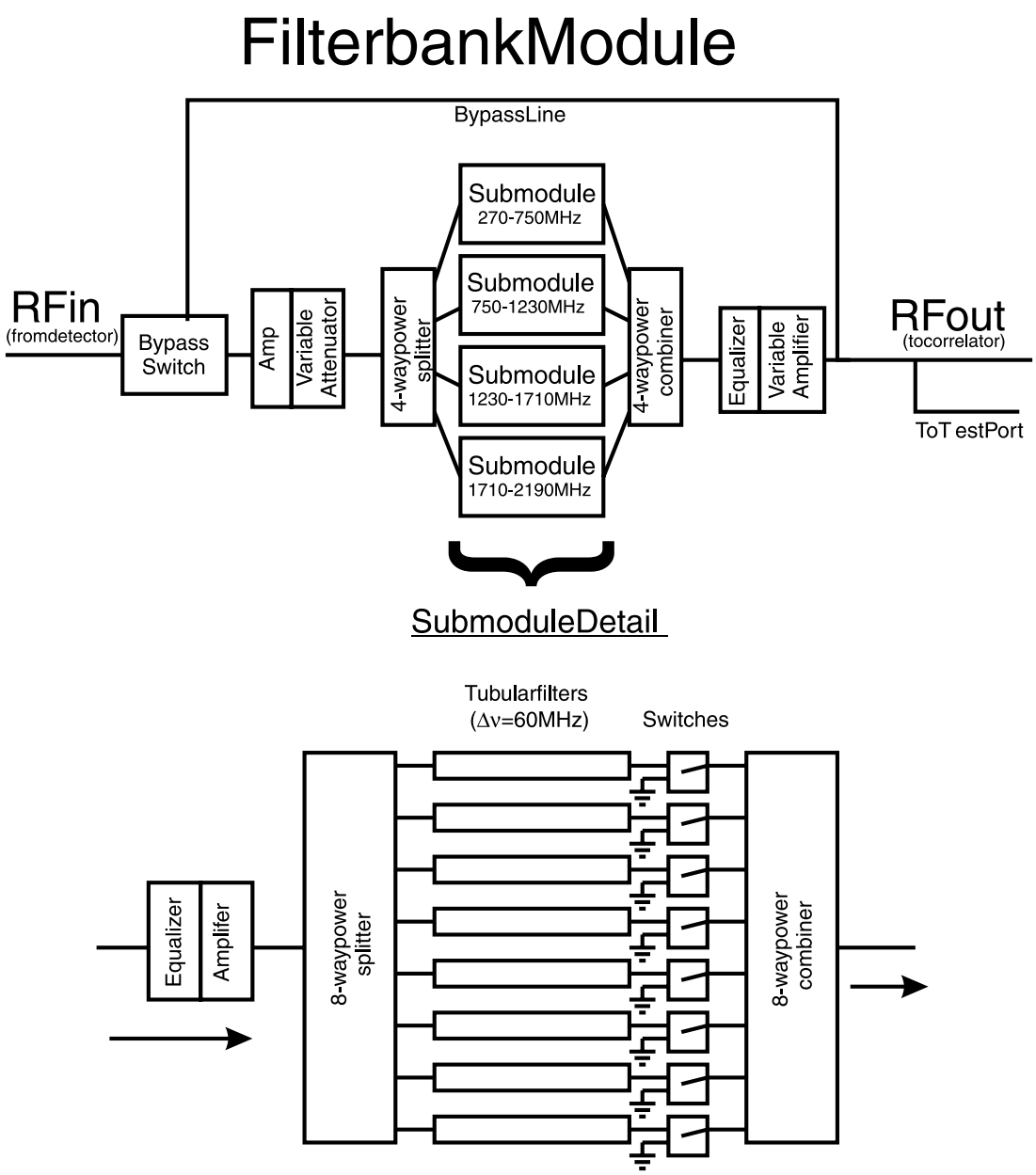


FIG. 2.—Block diagram of one of the filter-bank modules; there is one per telescope

parison or chopping (sometimes five), all easily controlled through a combination of hardware and software.

1. The sky signal is chopped at 150 Hz against a cold load to measure the infrared signal from the sky and to minimize the effect of low-frequency noise in the detection system.
2. The filter bank switches between BP0 and BP1 at 2.0833 Hz in order to calibrate out seeing and guiding changes.
3. The telescope nods 5″ on either side of the star every 15 s to measure the changing thermal background of the atmosphere and telescope optics.
4. The flat spectrum of the hotbody source (373 K) is observed every 5 minutes to measure the overall (frequency-dependent) gain of the ISI system, precisely calibrating the IR power ratios in BP0 to BP1.
5. When using lasing transitions of the $^{12}CO_2$ molecule, a final calibration is made for telluric absorption of $^{12}CO_2$. This is done by repeating these IR power ratio measurements on the star but using a nearby transition of the $CO_2$ laser LOs, one which has no known molecular line coincidences within the filter-bank bandpass. Note that the atmospheric optical depths for the $^{13}C$ isotopes are negligible.

IR total power data taken in the above manner are analyzed using an Interactive Data Language (IDL) reduction package that automatically separates out the various signals and returns a calibrated IR power ratio of BP0 with respect to BP1.

## 4. SPECTROSCOPY RESULTS

As previously emphasized, the lack of multiplexed readouts makes the acquisition of full-bandwidth, high-resolution spectra very time consuming. Hence, a series of strategic observations were planned to test robustly the experimental methodology and to confirm calibration reliability. A deep and broad $CO_2$ absorption line of the

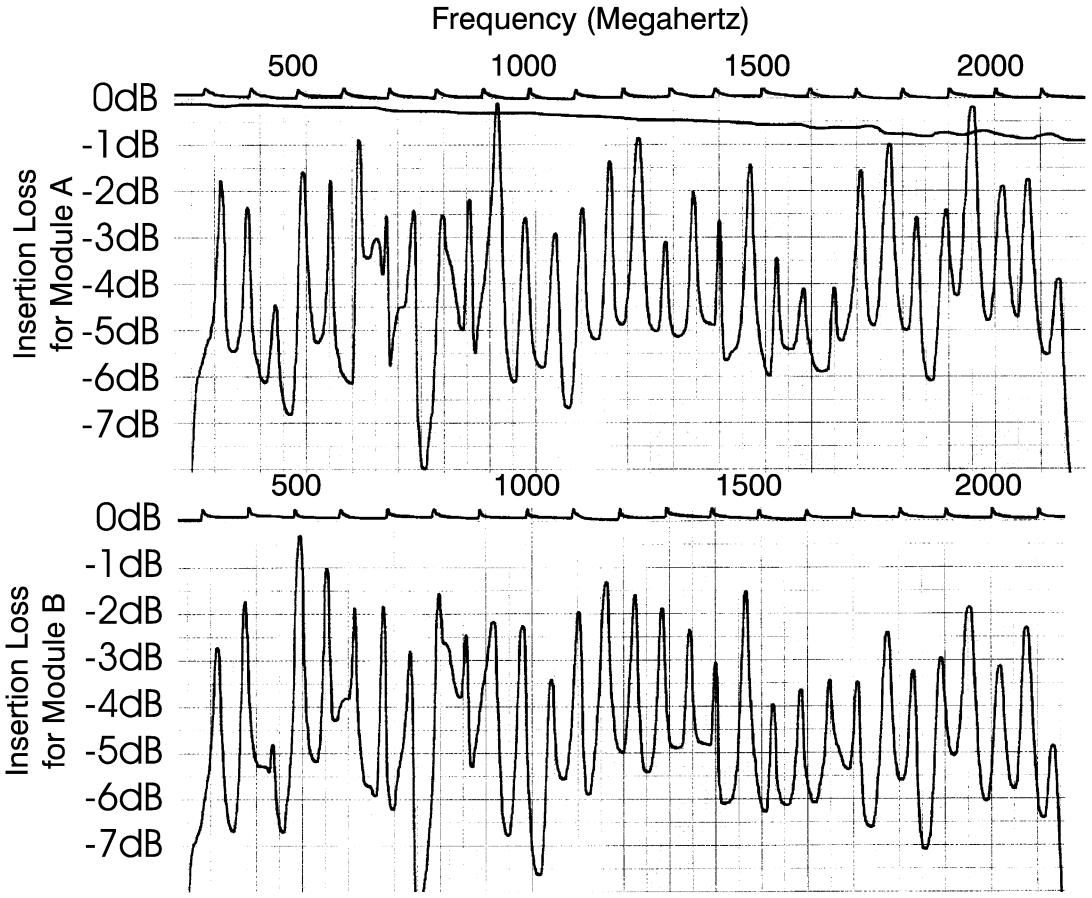


FIG. 3.—Filter-bank transmission (or insertion loss) as a function of frequency for both filter-bank modules. The two horizontal lines with tick marks define the frequency scale in steps of 100 MHz. The nearly straight line with small slope near the top of the figure is the transmission of the cables connecting to the filter-bank modules. The top curve (with the large ripple) corresponds to module A (plus connecting cables) used in telescope 1, while the bottom curve is the frequency response of module B used in telescope 2. Ideally these spectra should be flat, but improper overlap of neighboring filter bandpasses causes a $\pm 2.5$ dB bandpass ripple (see § 2.3).

Martian atmosphere and a single $NH_3$ absorption line of IRC +10216 were observed for these purposes, with results described below.

### 4.1. *Mars*

Deep absorption lines of Mars have previously been measured with a heterodyne spectrometer using a $CO_2$ laser as an LO by Betz (1977). The mid-infrared spectrum of Mars arises from thermal emission of the warm surface, heated by the Sun. Since the atmosphere of Mars is composed largely of $^{12}CO_2$, deep absorption lines are formed when viewing the surface through this molecular blanket. Mars is roughly

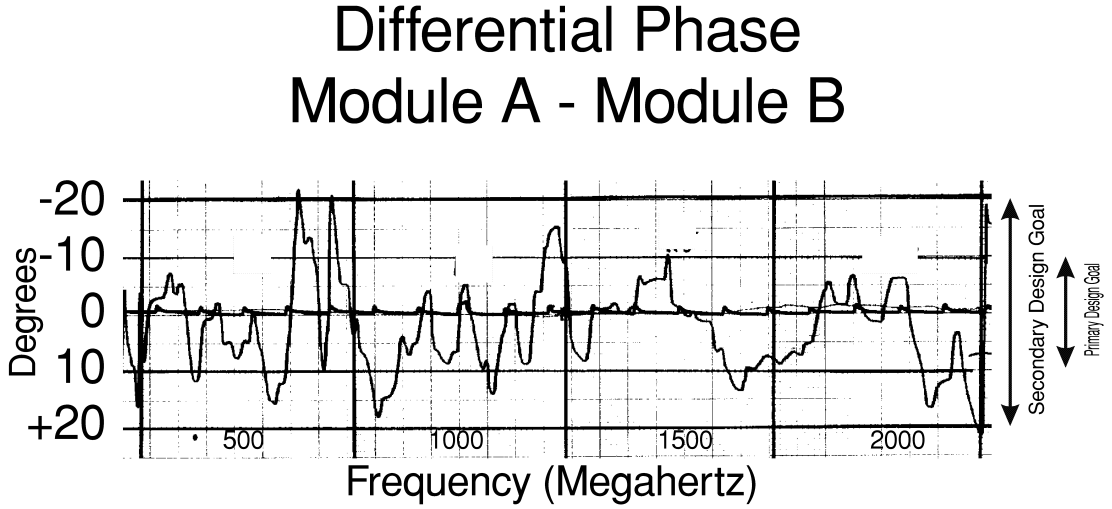


FIG. 4.—Relative phase response of the two filter-bank modules as a function of frequency. The bandpasses are matched to within 10° over 80% of the bandwidth and always within 20°.

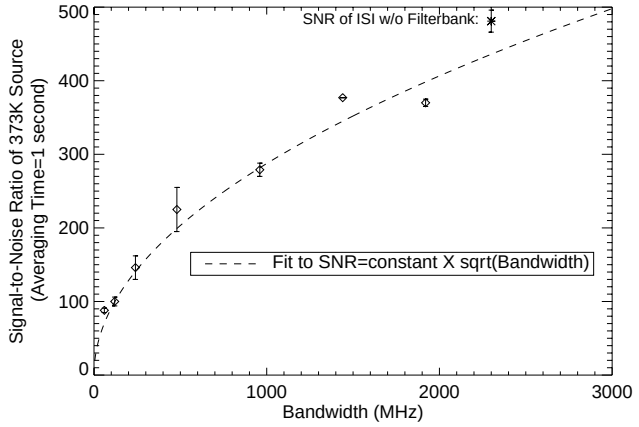


FIG. 5.—Plot of S/N for observations of a 373 K blackbody with and without the filter bank. This confirms that the system is shot noise limited and that the filter bank degrades the sensitivity by about 10% as expected.

as bright as IRC +10216, the brightest stellar mid-infrared source, and its pronounced spectral features present an ideal test case for calibration and checks of observing methodology.

Mars was observed on 1996 November 8 (UT), with the ISI lasers tuned to the P(16) transition of $^{12}C^{16}O_2$ at 10.55 $\mu$m. Combinations of four consecutive filters ($\Delta\nu = 240$ MHz) were observed across the entire ISI bandwidth to map out the spectral shape of the $^{12}C^{16}O_2$ P(16) absorption in the atmospheres of Mars and Earth. In each case, the narrow four-filter set was compared to the full bandwidth of the filter bank by frequency switching at 2.0833 Hz ($\tau = 480$ ms; see § 3) and integrating for $\sim$5 minutes. Figure 6 (*top panel*) shows the measured IR power in each of the four-filter bandpasses relative to the average of the entire continuum. The presence of the Martian $CO_2$ line near 1400 MHz is superimposed on a shallower, broader absorption feature attributed to the telluric absorption. Since the ISI is not able to separate the upper and lower sidebands, the $\sim$50% DSB depth of the Mars absorption line corresponds to nearly 100% absorption in a single sideband. This "folded" spectrum can be decomposed into the two sidebands by use of a model for the spectral shape.

After decomposition, the DSB spectrum in Figure 6 (*top panel*) is represented by a superposition of two Gaussian absorption features on a flat continuum. The center of one Gaussian is fixed at 0 MHz to fit telluric absorption, while the other Gaussian center is left free to fit the location of the Mars absorption core. The fitting procedure compensates for the relatively low spectral resolution (240 MHz) by smoothing the candidate DSB spectrum before folding and comparing to the data. The result of this fit, shown in the bottom panel of Figure 6, is in good agreement with expectations. The line center of the Mars line can be predicted based on the relative velocity of Mars with respect to Earth along our line of sight. NASA ephemerides predict a relative velocity of $-14.54$ km s$^{-1}$ on the date of observation. The corresponding Doppler shift is 1378 MHz at 10.55 $\mu$m, which is in good agreement with the best-fitted center of 1380 MHz.

### 4.2. *IRC +10216:* $NH_3$ *aQ*(2,2)

The observation of Mars convincingly demonstrated spectral line observations with the ISI and this filter bank.

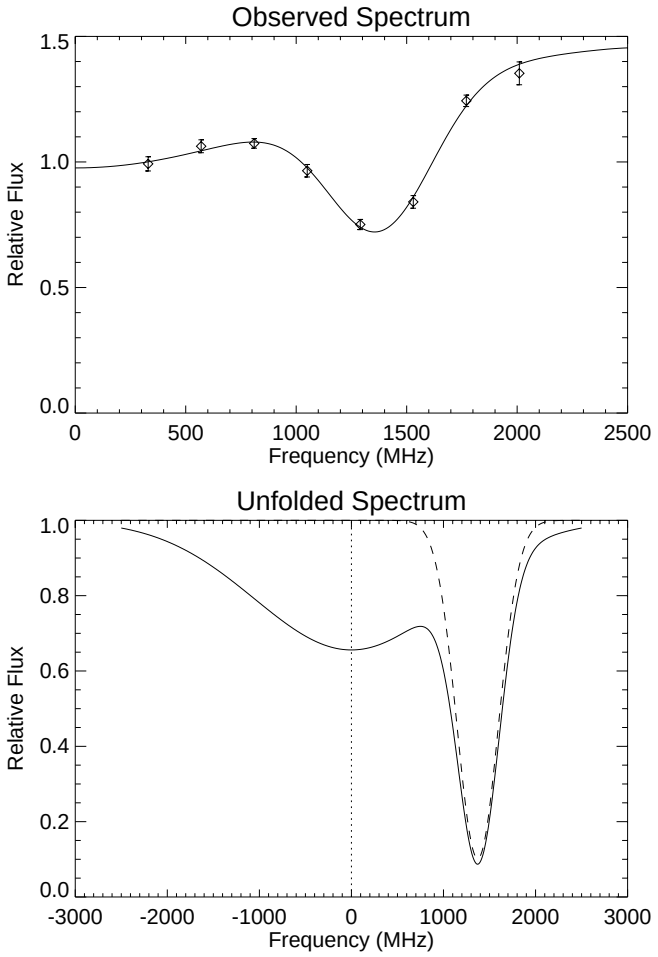


FIG. 6.—*Top panel:* Mars observation of P(16) transition of $^{12}CO_2$ on 1996 November 8. *Bottom panel:* Two-Gaussian model of the (unfolded) DSB spectrum. The wide Gaussian centered at zero frequency comes from telluric absorption, while the narrow, shifted feature is from the atmosphere of Mars itself. The relative velocity of Mars during this observation was $-14.54$ km s$^{-1}$ (1378 MHz at 10.55 $\mu$m).

However, for observation of narrow stellar lines, one must *very* precisely compensate for the orbital motion of Earth (Doppler shifts due to Earth's rotation are slightly less than the resolution of the filter bank and are neglected). Software to predict molecular-line Doppler shifts that had previously been used for the heterodyne measurements of AGB stars in the 1980s (Goldhaber 1988) was provided by A. L. Betz.

Two test observations of IRC +10216, separated by 2 weeks, were made in spring of 1997. The observations were separated in time to allow Earth to move along its orbit enough for a detectable shift in the line position to occur. Furthermore, since the chosen line had been previously observed by Goldhaber (1988), these observations would test whether the line depth has remained constant over the last decade. Both observations employed combinations of two filters that resulted in a spectral resolution of 120 MHz, just small enough to resolve the line as it appeared in Goldhaber (1988; $\sigma \sim 150$ MHz). Figure 7 shows the results of these observations from 1997 May and June.

Gaussian absorption features, smoothed to the 120 MHz resolution of this observation, were fitted to the data, and the line-center frequencies were determined. Table 2 shows the observed line-center locations and the theoretical predictions. The agreement is excellent and justifies interfero-

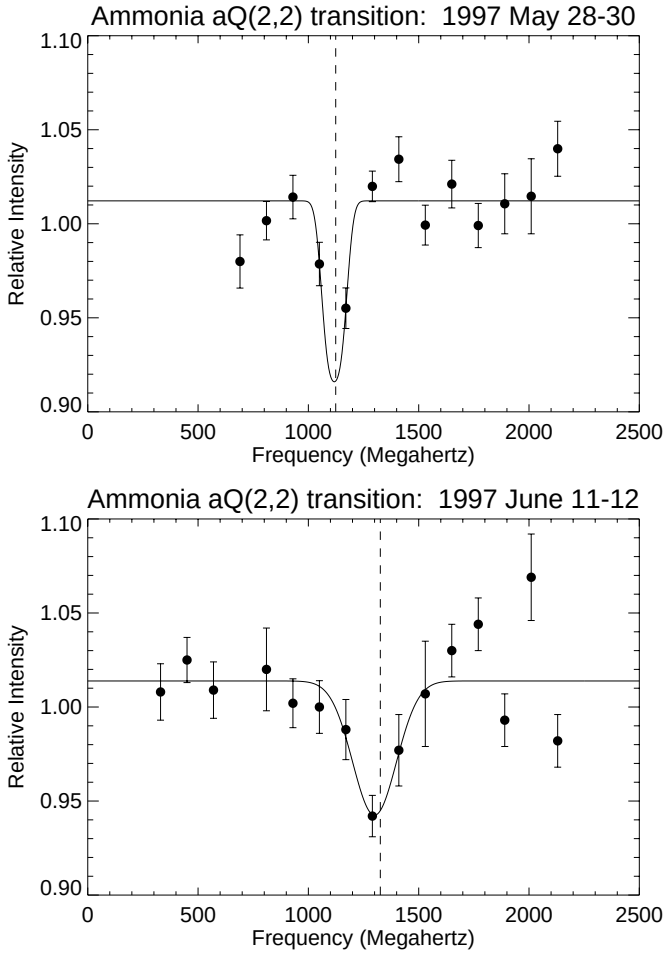


FIG. 7.—*Top panel:* Observation of aQ(2,2) transition of $NH_3$ around IRC +10216 on 1997 May 28–30. *Bottom panel:* Observation of aQ(2,2) transition of $NH_3$ around IRC +10216 on 1997 June 11–12. Single-Gaussian fits to the absorption profiles are shown. The vertical dashed line in each panel marks the predicted location of the absorption core, based on previous observations. Because of Earth's orbital motion, there is a frequency shift between observations that is clearly detected.

metric observations in the cores of previously observed lines with confidence in the calculations. The line detection in May was only marginal, but the movement of the absorption core is clear. While poorly determined, the apparent line widths and depths are consistent with the previous measurements of Goldhaber (1988).

### 4.3. *Final Calibration Check*

One further set of tests was performed to determine the accuracy of the IR power ratio measurements. The infrared power ratio in two different filter-bank bandpasses, denoted by BP0 and BP1, was measured in fall of 1998 on eight separate occasions while observing featureless stellar spectra (i.e., no known line coincidences). The average IR power of the full data set in BP0 compared to BP1 was $0.996 \pm 0.005$, consistent with unity.

TABLE 2

TEST OF SOFTWARE THAT CALCULATES DOPPLER SHIFTS OF CELESTIAL SPECTRAL LINES: $NH_3$ aQ(2,2) AROUND IRC +10216

| Date (UT) | Observed Absorption Core Location (MHz) | Predicted Absorption Core Location (MHz) |
|---|---|---|
| 1997 May 28–29..... | 1117±8 | 1124 |
| 1997 Jun 11–12..... | 1299±35 | 1326 |

## 5. INTERFEROMETRY ON SPECTRAL LINES: METHODOLOGY

Previous sections discussed the methodology of taking infrared power measurements on and off a spectral line. However, to perform interferometry, the fringe signal must be measured on and off the line as well. Measurements of the fringe power ratio on and off a spectral line can be combined with the IR power ratio measurements to yield the *visibility* ratio (VR) on and off the line, according to the formula (Hale et al. 2000)

$$\mathrm{VR} = \sqrt{\frac{\mathrm{FPR}}{\mathrm{IRPRT1} \times \mathrm{IRPRT2}}}, \qquad (1)$$

where FPR is the fringe power ratio, IRPRT1 is the infrared power ratio in telescope 1, and IRPRT2 is the infrared power ratio in telescope 2. This section will detail the methodology for obtaining a well-calibrated fringe power ratio using the ISI filter-bank system.

### 5.1. *Frequency Switching* (*Bandpass Chopping*)

As with the IR power ratio, for fringe power measurement the ISI filter bank is preset so that a narrow bandpass is selected to coincide with the core of a molecular absorption feature; this bandpass is referred to as BP0. A broad bandpass away from the absorption core, BP1, is selected as a reference. BP1 is generally much larger than BP0, so that shot noise in the BP0 measurement is the dominant noise term in the ratio of BP0 to BP1. A switching signal, generated and recorded by the real-time computer, is used to chop between these two bandpasses.

The frequency switching rate is adjustable and can be slowed to take advantage of good seeing conditions. In ordinary seeing conditions, a switching period of 240 ms is used, hence each bandpass is observed for blocks of 120 ms at a time. Even during poor atmospheric conditions, this provides for accurate calibration of fringe amplitudes and (relative) phase, allowing shot noise (in BP0) to dominate the measurement error of the fringe power. For observing nights with excellent seeing, a slower frequency switching rate allows longer coherent integration because of the longer atmospheric coherence time. In these cases, a 480 ms switching period was typically used.

For observations of an absorption line, the LOs were tuned to the appropriate lasing transition to bring the target molecular transition into the RF bandpass of the ISI detectors. Frequency switching was initiated and the correlator output voltage recorded (at 500 Hz) for an observation lasting approximately 5 minutes.

### 5.2. *Delay-Line Gain Correction*

As with any interferometer, the ISI uses a variable "delay line" to compensate for the changing geometric delay of the light coming from a source moving across the sky. While an automatic gain control circuit has been implemented in the delay line to keep the average transmission constant as the delay length changes, the spectral shape of the transmission

does not remain precisely constant. The frequency-dependent transmission (or "gain") of the delay line can change by 5%–10% over the course of a few minute observation, with a direct dependence on the specific length of delay in place. As can be seen in Figure 1, the filter bank is located in the RF chain *after* the delay line, and hence these changes corrupt the desired measurement of the fringe amplitude ratio on and off the spectral line. On the 4 m baseline, which was used for most of the filter-bank observations, the delay line changed every 20–60 s, depending on the source elevation. The associated spectral changes had to be calibrated in order to achieve accurate calibration of the fringe amplitude ratio of BP0 to BP1.

A real-time module was written and incorporated into the ISI delay-line software in the control computer for this purpose. When activated, this code instructs the data acquisition program to record into a file the exact time and settings of the delay line during an observation. After each $\sim 5$ minute measurement, the frequency-dependent gain changes of the delay line were immediately calibrated. This was done by observing a known flat continuum source (the ISI hotbody source at 373 K) and measuring the IR power in BP0 and BP1 while cycling through the just-used delay-line settings. While this method corrects for variations in the gain amplitude of the delay line, it does not correct possible phase mismatches that, if more than $\sim 20°$, cause residual miscalibration in the fringe amplitude in BP0 with respect to BP1. Calibration of this effect is discussed in the next section.

### 5.3. *Correlator Drifts/LO Switching*

Extensive engineering observations during fall of 1997 and spring of 1998 revealed that the spectral response of the fringe measurement, or correlator circuitry, showed drifts on the timescale of 0.5 hr, unrelated to the delay-line settings. Despite significant engineering efforts, the source of these variations could not be controlled, and one additional calibration procedure was adopted. Observations of a stellar source with a featureless spectrum were required for an absolute calibration of the fringe amplitude ratio on and off a spectral line (BP0/BP1). After each 5 minute observation on the target spectral region using the appropriate laser LO line, the LOs were adjusted to a neighboring lasing transition and the process repeated. Hence, interleaved observations were obtained under identical conditions except for the LO wavelength (which differed by $\sim 0.015$ $\mu$m). The true ratio of fringe amplitude in BP0 to BP1 is then the BP0/BP1 ratio at the target LO wavelength divided by the BP0/BP1 ratio at the calibration LO wavelength. This method ("LO switching"), while involving much off-source integration and repeated adjustments of the laser grating in order to change the laser frequency to the alternating transitions, is extremely robust and has no known systematic biases.

### 5.4. *Software for Analysis of Fringe Data*

Custom software written in IDL was used to read the recorded correlator voltage and bandpass-switching signals. This software took a power spectrum of each separate (usually 120 ms) block of fringe data for BP0 and BP1. The fringe power was measured around the fringe frequency (100 Hz), and the broadband noise signal was subtracted by sampling symmetric frequency bins $\sim 20$ Hz on either side of the main peak. Careful measurements during the engineering phase of the filter-bank commissioning established the noise power spectrum after the correlator circuit to be linear with frequency around 100 Hz to within 0.5%. Data for each delay-line setting were then collated and separately calibrated.

The mean and standard deviation of the fringe power in each bandpass and for each delay-line setting were then determined by a simple bootstrap analysis (see Monnier 1999 for more details). In addition, the fringe phase in BP0 can be subtracted from that measured in BP1. The frequency switching was rapid enough to eliminate atmospheric variations, essentially "freezing" the atmosphere, and the relative fringe phase in BP0 with respect to BP1 can hence be properly averaged (in the complex plane), a form of "phase referencing." After a total of a few nights of observing time on IRC +10216 using a narrow bandpass of about 180 MHz ($\Delta\lambda \sim 0.00007$ $\mu$m), the visibility amplitude ratio of BP0 to BP1 was measured to a precision of $\sim 1\%$ and the relative fringe phase to less than a few degrees. The first interferometric results on spectral lines are presented in Paper III of this series.

## 6. CONCLUSIONS

An RF filter bank has been constructed and used with the ISI interferometer. The ISI filter bank functions well as a spectrometer, although the data rate is low. The filter-bank system was not designed to be an efficient spectrometer, but rather to be an effective first-generation tool to harness the spectral resolving power of the ISI for interferometry. The observations presented here confirm the ability of the ISI to do such work, and an observing methodology for combining interferometric observation with filter-bank observation has been outlined. This methodology has been used successfully for observing fringe visibilities on and off a number of molecular absorption lines. Preliminary results are discussed in Monnier (1999), and a more complete analysis follows in Papers II and III of this series.

This new capability of the ISI has so far been used to measure the location of molecular formation zones for $NH_3$ and $SiH_4$ around the carbon star IRC +10216 and for $NH_3$ around the red supergiant VY CMa. However, strong spectral absorption features of these same molecules could also be investigated for IRC +10420, *o* Ceti, and NML Cyg, whose line depths and shapes have already been measured (McLaren & Betz 1980; Betz & Goldhaber 1985; Goldhaber 1988). Measurements of angular diameters of red supergiants and Mira variables on and off their recently discovered mid-infrared water lines (Jennings & Sada 1998) are also potentially rewarding. These lines are thought to form in the stellar photosphere and may affect the interpretation of previous angular diameter measurements. The use of high spatial and spectral resolution line observations in between water lines could potentially allow the "true" continuum diameters to be measured, uncorrupted by line blanketing. Last, fine structure and recombination lines around some emission-line stars (e.g., MWC 349; Quirrenbach et al. 1997) can be observed using the $CO_2$ LOs and could make unique measurements of the emitting regions.

While the potential for interesting new results is rich, the nonmultiplexed output of this particular filter-bank system makes it very difficult to observe new sources in detail when the spectral line profiles have not been previously measured by a multiplexing spectrometer. The lines around some sources (*o* Ceti, for instance) have been observed to change

in time, and new spectra are essential for interpreting additional interferometric line data.

We want to recognize the computer programming of Manfred Bester and Carl Lionberger, which was essential for the filter bank to interface with the ISI control system. This work is part of a long-standing interferometry program at University of California, Berkeley, supported by the National Science Foundation (grants AST-9221105, AST-9321289, and AST-9731625) and by the Office of Naval Research (OCNR N00014-89-J-1583).

REFERENCES

Bester, M., Danchi, W. C., Hale, D., Townes, C. H., Degiacomi, C. G., Mekarnia, D., & Geballe, T. R. 1996, ApJ, 463, 336
Betz, A. L. 1977, Ph.D. thesis, Univ. California, Berkeley
Betz, A. L., & Goldhaber, D. M. 1985, in Mass Loss from Red Giants, ed. M. Morris & B. Zuckerman (Dordrecht: Reidel), 83
Betz, A. L., Johnson, M. A., McLaren, R. A., & Sutton, E. C. 1976, ApJ, 208, L141
Danchi, W. C., Bester, M., Degiacomi, C. G., Greenhill, L. J., & Townes, C. H. 1994, AJ, 107, 1469
Goldhaber, D. M. 1988, Ph.D. thesis, Univ. California, Berkeley
Hale, D. D. S., et al. 2000, ApJ, 537, 998
Holler, C. 1999, M.A. thesis, Ludwig-Maximilians-Universität
Isaak, K., Harris, A. I., & Zmuidzinas, J. 1999, in ASP Conf. Ser. 156, Highly Redshifted Radio Lines, ed. C. L. Carilli, S. J. E. Radford, K. M. Menten, & G. I. Langston (San Francisco: ASP), 86
Jennings, D. E., & Sada, P. V. 1998, Science, 279, 844
Lipman, E. A. 1998, Ph.D. thesis, Univ. California, Berkeley
McLaren, R. A., & Betz, A. L. 1980, ApJ, 240, L159
Monnier, J. D. 1999, Ph.D. thesis, Univ. California, Berkeley
Quirrenbach, A., Thum, C., Martin-Pintado, J., & Matthews, H. E. 1997, BAAS, 191, 4719
Thompson, A. R., Moran, J. M., & Swenson, G. W. 1986, Interferometry and Synthesis in Radio Astronomy (New York: Wiley-Interscience)